This article has been accepted for publication in a future issue of this journal, but has not been fully edited. Content may change prior to final publication. Citation information: DOI 10.1109/JSTQE.2018.2873489, IEEE Journal of Selected Topics in Quantum Electronics

Quantitative Evaluation of Skin Surface Roughness Using Optical Coherence Tomography *In Vivo*

Sanzhar Askaruly, Yujin Ahn, Hyeongeun Kim, Andrey Vavilin, Sungbea Ban, Pil Un Kim, Seunghun Kim, Haekwang Lee, and Woonggyu Jung

***Abstract*— The quantitative monitoring of skin topography is important in the field of cosmetics and dermatology. The most widespread method for determining skin roughness *in vivo* is to use skin microrelief, PRIMOS device, which allows a noninvasive, fast and direct measurement of the skin surface. However, it has drawbacks, such as the interference of backscattering from volumetric skin and motion artifacts. In this study, we demonstrate the potential of OCT for providing reliable and quantitative skin surface roughness. In order to evaluate the performance of OCT for skin surface analysis, different types of skin phantoms are fabricated and measured. We utilize OCT to identify the effect of cosmetics as well as human skin topology for various aging groups and different skin regions. Skin surface roughness parameters based on ISO 25178 part 2 standard definitions are then derived from home-built image processing software and compared with one acquired from PRIMOS. Our results show that skin surface geometry acquired from 3D OCT images is well quantified to complex wrinkle structure and robust to the angle of the subject. Since OCT enables to present quantitative skin topology and volumetric skin anatomy simultaneously, it would be a useful tool to deliver comprehensive and intuitive information in dynamic skin observations.**

***Index Terms*— Tomography, Biomedical image processing, Surfaces.**

I. Introduction

THERE has been an enormous expansion in the cosmetics market due to anti-aging skin care along with accelerated innovation and development of more effective skin products [1], [2]. According to an Orbis Research report, it is estimated that the global anti-aging cosmetic market will reach a value of $331.41 billion by 2021 [3]. Cosmetics companies, in pursuit of their competition, are currently driven to develop not only high quality skin products, but also high standard product assessment instruments which offer reliable and fast feedback of skin conditions such as structure and roughness. In particular, the *in vivo* and quantitative observation of skin is required for an accurate assessment of the effectiveness of an anti-aging product. To date, various techniques have been applied in order to monitor the morphological change in skin. The use of skin replica or reprints with optical profilometry is the most common and simple way to observe skin topology [4], [5]. However, this method is inadequate when *in vivo* and fast feedback is required, because it is an indirect measurement and its outcome can be affected by air-bubbles [6]. Recently, advanced optical imaging modalities, such as reflectance confocal microscopy, fluorescence and second-harmonic microscopy, have been suggested to be promising tools for skin tissue analysis [7]-[9]. In each of these techniques, pathologic changes in cellular, nuclear morphology, and melanin content are clearly observed. Even though they provide high-contrast and cellular resolution imaging, the limitation in the field of view (FOV) or contrast remains a critical restriction for wrinkle investigation. One of the most commonly used imaging systems for skin measurement, PRIMOS (Canfield, US), has been proposed as an objective tool in the cosmetics industry for studying skin topography and the volume of wrinkles. PRIMOS is a non-invasive, fast and direct measurement of the skin surface with high precision [10]. It has been successfully tested in scar assessment applications [11]. However, PRIMOS has difficulty in providing accurate and reliable skin analysis because its results can vary according to orientation, motion artifacts, as well as back scattering of the subject [12].

Optical coherence tomography (OCT) has emerged as an appropriate tool for skin analysis with various advantages including cross-sectional, high-resolution, and real-time tissue imaging [13], [14]. In particular, the technical performance of OCT, such as 3D volumetric and deep imaging capability, could avoid the critical drawback of PRIMOS such as the dependency of wrinkle orientation. OCT inherently maintains essential advantages for ideal skin imaging and is a promising tool for robust and accurate measurements during *in vivo* studies of skin. Although being widely utilized in biomedical applications, such as detecting skin tissue abnormalities [15], [16] and laser wound healing monitoring [17], [18], only few OCT studies have assessed the aging of the skin surface and quantitative analysis [19]-[21]. Herein we demonstrate the potential of an OCT device that concentrates on robust and reliable wrinkle analysis toward quantitative aging study in dermatology and cosmetic applications.

This article has been accepted for publication in a future issue of this journal, but has not been fully edited. Content may change prior to final publication. Citation information: DOI 10.1109/JSTQE.2018.2873489, IEEE Journal of Selected Topics in Quantum Electronics

II. Materials and Methods

A. *Optical coherence tomography (OCT)*

We utilized a swept source optical coherence tomography (SS-OCT) for the *in vivo* evaluation of the skin wrinkle analysis. The swept source laser (Axsun Tech.) was operated at a 1310 nm center wavelength with a tuning range of 110 nm at a rate of 100 kHz, providing an axial resolution of ~7 μm. The sample unit of our home-built SS-OCT system consisted of a collimator, a galvanometer scanner, and an objective lens with a lateral resolution of ~15 μm. Two beams returned from each sample and the reference unit are interfered by Mach-Zehnder interferometry, which was converted to an electrical signal by a balanced amplified photodetector (PDB450C, Thorlabs Inc.). And then, the digitizer (ATS9350, AlazarTech Inc.) digitized the electrical signals for plotting intensity-based images as shown in Fig. 1(A).

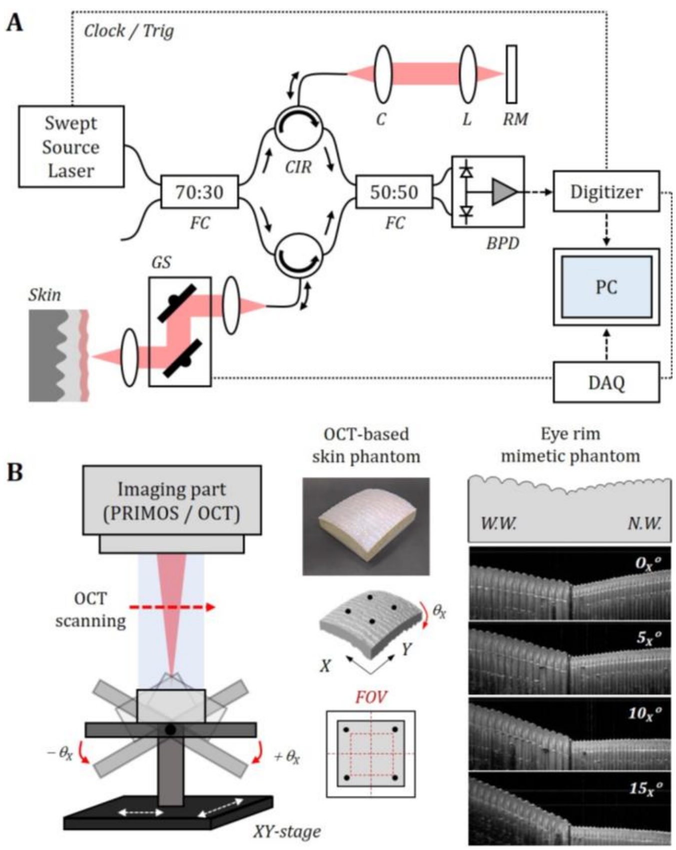

Fig. 1. (A) Schematic diagram of the SS-OCT system used for scanning skin wrinkle. FC: fiber coupler, CIR: circulator, GS: galvanometer scanner, C: collimator, L: lens, RM: reference mirror, BPD: balanced photodetector; (B) Method for image acquisition by PRIMOS and OCT at different angular position using 3D printed skin phantoms.

B. *Measurement of skin phantom and human skin*

The roughness analysis of phantom at different angular position and skin structure was executed by using OCT and PRIMOS (GFM GmbH, Germany). In this experiment, we used two kinds of skin phantoms, which were produced by a commercial 3D printer (Fortus 250mc, Stratasys Ltd.). First phantom was made for implementing the real human skin structure as shown in Fig. 1(B). It was based on *in vivo* 3D OCT image data of human skin which was converted to stereo-lithography file for enabling 3D printing. OCT-based skin phantom was fabricated with 4× magnification and imaged by OCT again to confirm the similarity with OCT images. Since this phantom was constructed with large scale to real skin, its structure of wrinkles showed less compact with low frequency in terms of intervals. Another phantom was built for mimicking the eye rim structure which has different intervals of wrinkle patterns and surface curvatures; narrow winkle (N.W.) and wide winkle (W.W.), as shown in Fig. 1(B). The frequency of wrinkle pattern was higher than one on the OCT-based skin phantom. In comparison study, two types of phantoms were mounted on 2 axes optical moving stages with rotator to align the center. The wrinkle morphology of constructed skin phantoms was then imaged by OCT and PRIMOS with different angular positions.

For *in vivo* study, human subjects for the skin test were divided into two groups. In the first group, 10 people (35.3 ± 8.5 years old) were randomly selected and their skins were examined by SS-OCT (Result 3.2). In the second group, we recruited a total of 10 human participants, who were then divided into two different groups by age. 5 people in a young age group (27.2 ± 1.2 years old) and 5 people in an old age group (55.4 ± 6.9 years old) were separately examined to analyze the changes of any wrinkles (Result 3.2). Before imaging procedure, the region of interest of the skin was marked and washed by cleansing cream and exposed to a constant temperature and humidity in order to stabilize the experimental conditions. For OCT and PRIMOS imaging experiment, we utilized a product of cover-up makeup (Verite, Amorepacific. Corp.) incidentally to monitor and quantify the change of wrinkle morphology *in vivo*. All the research procedures using human participants were carried out at Amorepacific Corp. R&D center in tight accordance with the Institutional Review Board for Protection of Human Subjects in Research (IRB) approval (2017-1CR-N029S).

C. *Image processing*

There are several algorithms that detect the boundaries between the human skin subsurface layers in OCT images. Mostly, these were developed for the investigation of epidermal thickness. Specifically, the shapelet-based image analysis technique for skin measurement fails to closely follow all the contours in wavy structures [22]. As reported, this is due to shapelet kernel, which is only processed in a single direction, normal to the skin surface. Another technique of automatic measurement of epidermal thickness has been reported *via* analysis of intensity profile [23]. However, A-scan results are unable to take into account the effect of line and wrinkle features in skin structure. Other more complex techniques, such as segmentation by classification of speckle statistical parameters and graph-based skin surface detection were also proposed to accurately indicate boundaries [24], [25]. However, intensive calculation time has limitation to apply it in practical use. In this study, we developed an automatic segmentation algorithm to detect skin surface using MATLAB, as illustrated in Fig. 2.

The overall process of detecting the surface consists of two steps: (1) Curvature estimation and (2) Surface detection after flattening method. Being characteristics of any skin surface, the natural curvature of skin serves as undesirable artifact which might lead to miscalculations of real values of roughness. It is because that this parameter could be correlated with amount of deviations from average line in wrinkles. In first image processing step for estimating skin curvature, we initially performed Gaussian filtering to diminish the effect of speckle noise inherently present in OCT images. Next, using a median filter, a smoothed image with a diminished effect from noise was obtained while preserving the edges of the original image. We further applied a differential filter to emphasize the ideal surface boundary. The ideal surface was finally detected by finding the minimal intensity values from the results of the differential filter procedure. The determined ideal line serves as a reference for producing flatten OCT image. Similar to previous step, the real skin surface could be highlighted with differential filter procedure. Finally, the last subfigure in the lower row presents the performance of the algorithm by overlaying the detected real surface onto the original normalized image. The reported computation technique was carefully examined on the image dataset consisting of more than 15,000 images and its acceptable efficiency to robustly identify the skin surface was confirmed on every input image.

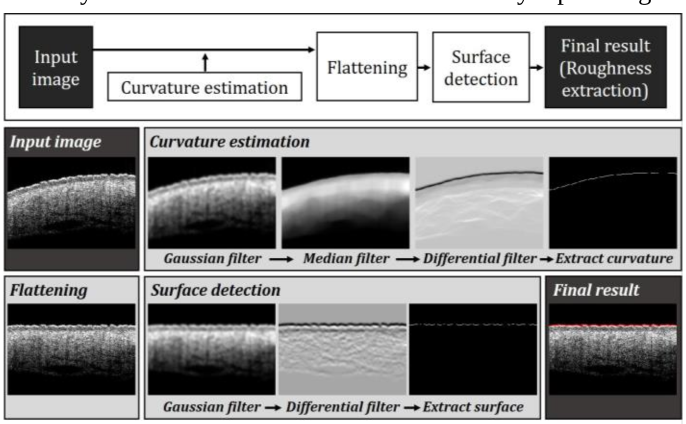

Fig. 2. Procedure of automatic skin surface detection algorithm for quantitative analysis of skin roughness. The process includes 'Curvature estimation' and 'Surface detection after flattening' procedures.

Fig. 3 introduces the procedure of creating skin surface topology from volumetric OCT image. The initial 3D OCT image of skin was reconstructed by a batch of 500 two-dimensional images, which clearly identified the natural curvature of the skin surfaces as shown in Fig. 3(A). Applying aforementioned image processing using flattening process, resultant 3D OCT image as well as topological image from volumetric OCT of skin were extracted as presented in Fig. 3(B). The normalized wrinkle depth profile then denoted as color image map and corresponding probability distribution were derived as depicted in Fig. 3(C) and Fig. 3(D).

D. Quantification of surface roughness

Roughness characterizes irregularities on surfaces, providing information on the topography and geometry of different surfaces. These irregularities occurring within uneven surfaces, consisting of peaks and valleys, can be determined by

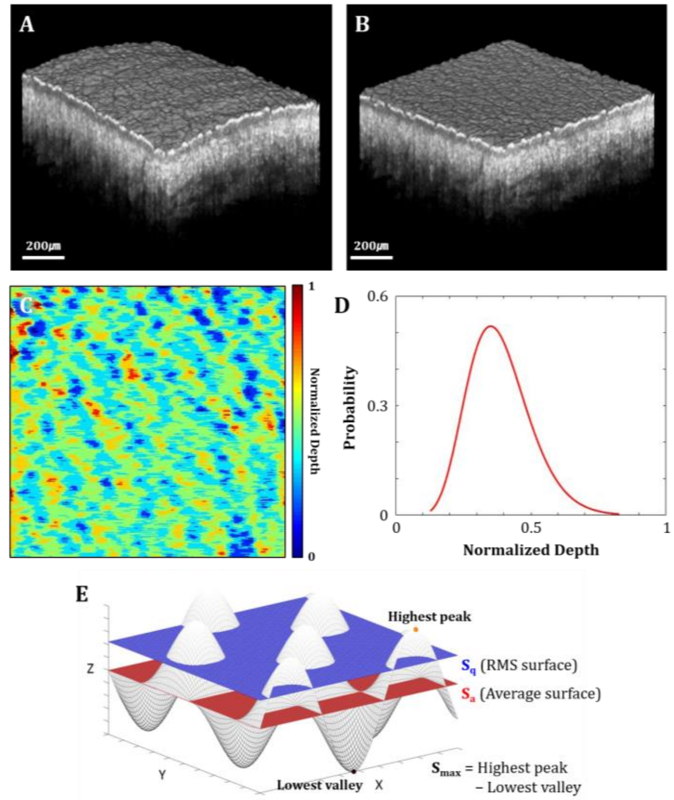

Fig. 3. Image processing and quantification of OCT image. (A) Original 3D OCT image of human skin; (B) Flattened 3D OCT image; (B) Surface topology acquired from 3D OCT; (D) Probability of depth profile; (E) ISO standard for extracting quantitative surface roughness.

measuring their height values. In this study, the skin surface roughness and geometry parameters within a sampling area were determined using ISO (International Organization for Standardization) 25178 part 2 standard definitions for arithmetic mean roughness (S_a), root mean square roughness (S_q) and maximal roughness of surface (S_{max}) within sampling area [26]. The sampling area is equivalent to the field of view (FOV) of OCT system setup, which is 10 mm x 10 mm.

Here, average surface roughness represents the arithmetic mean of absolute values of heights within the sampling area, described by Eq. 1.

$$S_a = \frac{1}{nx \times ny} \sum_{i=1}^{nx} \sum_{j=1}^{ny} \left| z(x_i, y_j) \right| \qquad (1)$$

with *nx* and *ny* being the sample lengths of cross-sectional views (total image pixel number), retrieved from reconstructed three-dimensional volumetric skin, and $z(x_i,y_i)$ are the corresponding vertical pixel distances from the mean line to the *i*th data or image pixel point in the *x* and *y* plane, see Fig. 3(E).

Root mean square surface roughness represents the root mean square value (RMS) of the surface heights shown in Fig. 3(E) and denoted by S_q .

$$S_q = \sqrt{\frac{1}{nx \times ny} \sum_{i=1}^{nx} \sum_{j=1}^{ny} z(x_i, y_j)} \qquad (2)$$

Finally, the maximum height of the surface is the difference between the highest peak and the lowest valley on the entire measuring field.

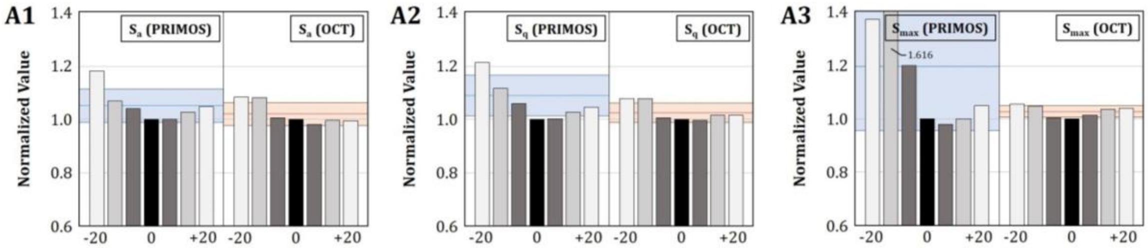

A1

	PRIMOS		OCT	
0°	1		1	
±10°	1.040	0.950	1.006	0.981
±15°	1.125	0.935	1.082	0.996
±20°	1.120	0.953	1.084	0.995

A2

	PRIMOS		OCT	
0°	1		1	
±10°	1.059	1.002	1.006	0.996
±15°	1.116	1.026	1.078	1.015
±20°	1.213	1.047	1.078	1.014

A3

	PRIMOS		OCT	
0°	1		1	
±10°	1.194	0.979	1.004	1.014
±15°	1.616	1.001	1.046	1.035
±20°	1.372	1.049	1.056	1.040

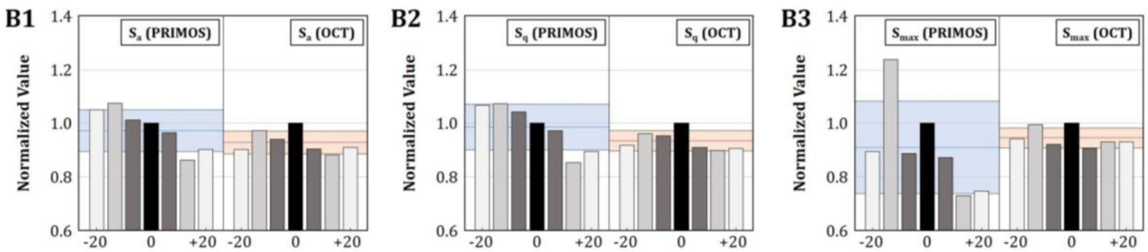

B1

	PRIMOS		OCT	
0°	1		1	
±10°	1.000	0.953	0.939	0.903
±15°	1.064	0.851	0.972	0.882
±20°	1.040	0.891	0.902	0.909

B2

	PRIMOS		OCT	
0°	1		1	
±10°	1.042	0.971	0.954	0.910
±15°	1.073	0.853	0.960	0.897
±20°	1.067	0.894	0.916	0.906

B3

	PRIMOS		OCT	
0°	1		1	
±10°	0.887	0.872	0.921	0.905
±15°	1.238	0.728	0.995	0.931
±20°	0.894	0.746	0.942	0.929

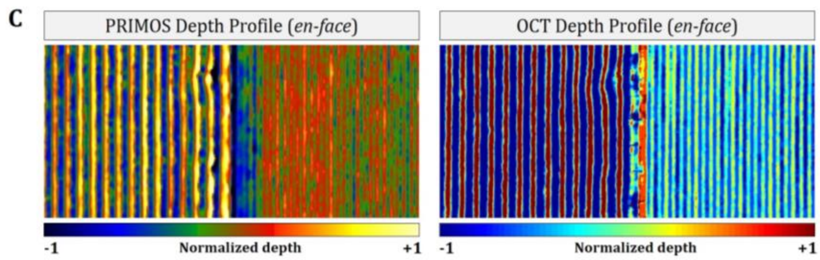

Fig. 4. Comparison study of normalized roughness values between PRIMOS and OCT at varied angular positions -20°, -15°, -10°, 0°, +10°, +15°, +20° for (A) OCT-based skin phantom and (B) Eye rim mimetic phantom. (C) Surface topology of skin phantom achieved by PRIMOS and OCT.

III. RESULTS

A. *Comparison study using skin phantom*

OCT and PRIMOS devices were compared regarding imaging capability in terms of delivering consistency. Specifically, an investigation into the ability to stay unaffected during sample fluctuation was conducted. We observed the presence of change in skin roughness results during the imaging angle variation for both devices. This evaluation is critical to perform since the experiment outcome should be consistent under different experimental circumstances. Moreover, subjects can accidentally twitch their skin region during examination, which is undesirable for acquiring quantitative results. In order to verify it, two kinds of 3D printed phantom fragments were created. First phantom was fabricated to describe the real human skin structure which was based on *in vivo* 3D OCT image. The size of phantom was magnified having 4 cm × 4 cm, which formed large-scale of wrinkle over real dimension. We imaged this phantom using OCT and PRIMOS varying the angular positions from - 20° to 20°. The values of skin roughness were then extracted by home-built software using surface flattening and software included in the PRIMOS package, respectively. Fig. 4(A) presents results of comparison study at 7 different angle positions for OCT-based skin phantom. As can observe from Fig. 4, the standard deviations at the left column of PRIMOS is higher than one in the right column of OCT. This outcome indicates that skin surface analysis with OCT offers more consistent performance despite the angle variation of subject. This is because that OCT measurement includes the surface tracking and flattening algorithm which is based on natural curvature extracting from volumetric and deep skin OCT imaging. On the other hand, PRIMOS uses only shallow surface profile which may induce erroneous results. This is the reason why PRIMOS results has more fluctuation at higher angle, 20° over 0° position. Another phantom was artificially designed and constructed as mimic of eye rim structure having narrow and wide wrinkle patterns within tight intervals. Eye rim mimicking phantom was imaged by OCT and PRIMOS in same condition and procedure as described above, and its outcome is shown as Fig. 4(B). Similar to the results of previous phantom study, OCT measurement

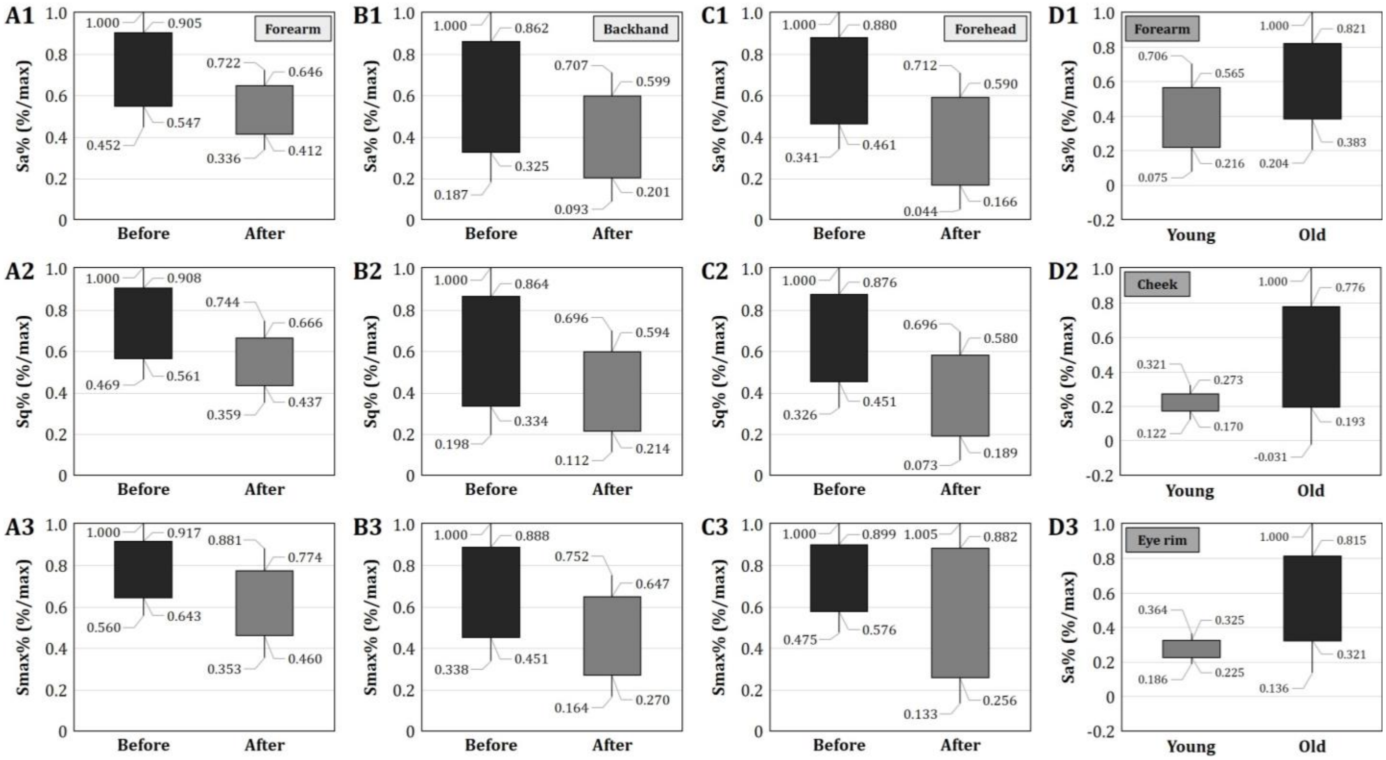

Fig. 5. (A)-(C) Skin surface roughness changes before and after applying cosmetics for forearm, backhand and forehead accordingly. (D) Distribution of average roughness values in young and old age group subjects for three skin regions

has more reliability over one acquired from PRIMOS. In order to observe the compact and periodic structure of wrinkle, imaging device requires high resolution which was evaluated as presented in Fig. 4(C). Topologic image of OCT is well defined periodic structures in two different wrinkle structures. On the contrary, topology achieved by PRIMOS visualizes unclear distinction and irregular pattern of surface which is more severe in high frequency wrinkle network. Through experiments with two phantoms we identified that OCT is not only a feasible device for investigating skin surface, but could also exceed PRIMOS in terms of resolution, accuracy and consistency under position variable conditions of subjects.

B. In vivo human study for measuring skin roughness

The influence of cosmetic products on changes in skin surface roughness was evaluated using OCT. In this study, we utilized a product of makeup which was spread on subject's skin in general use. Since it was the corrective cosmetics, our hypothesis was that the subject's skin should get smoother after applying it, showing a decrease in roughness values. Through this experiment, we could demonstrate that the quantitative monitoring using OCT can be a practical approach to evaluate the effectiveness of wrinkle care methods such as anti-aging ointments or medical skin treatment.

In this experiment, ten subjects of mixed age groups were engaged. For each subject, different regions of the body such as forehead, forearm and backhand were determined as our region of interest (ROI). Once cosmetics was used on skin, we could verify that wrinkles of subjects were less visible with eye inspection right after applying it. We closely investigated skin surface roughness parameters using OCT and PRIMOS. The numerical values of the conducted experiment are gathered into Fig. 5(A)-(C). In Fig. 5(A)-(C) each of the three columns represent the skin region of interest: forehead, forearm, and backhand accordingly. The rows in the figures represent the roughness parameters. We examined the average, RMS and total profile skin roughness. The values are normalized based on the initial skin roughness state without cosmetic use, depicted with black vertical bar graphs on the left. In contrast, the gray bar to the right represents the roughness values after applying cosmetics. From Fig. 5(A)-(C), it can be seen that the gray bars are lower than those in black. The effect implies that after applying cosmetics there is a tendency for the skin roughness value to decline. This validates our hypothesis and characterizes OCT as a viable skin analysis and treatment monitoring tool.

In further experiment, the change of roughness values and their correlation with subject age was examined. Through this study, we could estimate that quantification of wrinkle using OCT is helpful to understand the aging process and the various parameters affecting it. 10 human subjects of two age groups were involved. The first five subjects representing the younger generation (mean age: 27) and the other five subjects for the older generation (mean age: 55) were considered. The three-dimensional OCT images were acquired in three different skin regions. The same imaging procedure and experiment protocol were repeated for the cheek, eye rim and forearm skin regions. Table 1 represents the numerical values of the average, RMS and maximal profile roughness parameters. They are grouped according to their age group and the skin region being investigated. The numerical results from Table 1 suggest there are higher values in older subjects. In contrast, the younger representatives have reduced numbers for the same parameters. The outcome states the presence of a positive correlation between subject age and roughness parameters. Through this experiment, the influence of the aging process on skin surface roughness values was confirmed. Moreover, roughness values among various skin regions were compared as shown in Fig. 5(D). It suggests that there is the least notable difference between young and old age groups in the bar chart which corresponds to the forearm. On the other hand, looking at the cheek and eye rim there is greater difference in the value of the surface roughness distribution. Through these results, we confirmed that OCT could be potential device in order to monitor and quantify wrinkle variation by aging *in vivo*.

TABLE I
ROUGHNESS VALUES FOR YOUNG AND OLD AGE GROUPS

Age group	Skin region	Average	RMS	Maximal
Young	Forearm	0.49 ± 0.22	0.98 ± 0.30	5.70 ± 0.43
	Cheek	1.02 ± 0.23	2.08 ± 0.40	10.10 ± 2.33
	Eye rim	1.22 ± 0.17	2.34 ± 0.34	10.82 ± 2.27
Old	Forearm	0.78 ± 0.28	1.58 ± 0.67	8.05 ± 2.66
	Cheek	2.10 ± 1.07	4.23 ± 1.94	13.33 ± 3.08
	Eye rim	2.71 ± 0.82	5.22 ± 1.53	14.94 ± 1.32

IV. DISCUSSION

PRIMOS is a powerful device capable of performing noninvasive, fast and direct measurement of the skin surface, and rich functionality included in its software package. However, it has restriction to acquire information while preserving both high resolution and reliability despite its popularity.

In this study, we investigated potential of OCT for quantitative monitoring of skin surface roughness and presented a comparison of measurements with the PRIMOS. OCT clearly visualized morphologic variation of skin surface in three-dimensional and high-resolution approach. We found that OCT combined with flattening image processing was robust to evaluate quantitative skin roughness, while reducing image artifacts such as dependence onto wrinkle orientation or motion artifacts. Through our experiments, we also confirmed that OCT could deliver comprehensive and intuitive information of morphologic changes in the skin and roughness parameters for monitoring skin treatment and the influence of the further skin aging study.

In this manuscript, we mainly focused on quantitative estimations of actual roughness parameter values from detected surface topography. Advances in technology such as cubic meter volume OCT would make it possible to improve the image quality as well as applicability [27]. The implementation of better OCT contrast and imaging depth would help to accurately quantify the epidermal thickness properties as well. When the epidermal layer is clearly observed, a new algorithm needs to be proposed for the quantification of the roughness parameters in the dermal-epidermal junction [28]. The correlation of the dermal-epidermal junction roughness with the aging process is a relevant subject, since inner layers are less affected by the extrinsic environmental factor. Finally, the integration of high-speed OCT in a compact hand-held device could possibly make the procedure more time-efficient, opening up new opportunities to study skin in real-time [29], [30].

V. CONCLUSION

We have demonstrated the potential of OCT based on flattening image processing for monitoring quantitative skin roughness. Experimental results of phantom study show that OCT is reliable to the angle of the subject and compact wrinkle structure compared to one acquired from PRIMOS. We have also investigated that OCT is adequate for monitoring wrinkle morphology changes *in vivo*. Through our results, we have found that OCT would be a useful tool to deliver comprehensive and intuitive information in dynamic skin observations, since OCT enables observing quantitative skin topology and volumetric skin anatomy simultaneously. The integration of our tool with advanced OCT technology, which includes a hand-held probe and volumetric OCT system would create ideal opportunity to serve the routine process in the real-world dermatology or to enter cosmetics market.

ACKNOWLEDGMENT

This work was supported by a grant of the Korean Health Technology R&D Project, Ministry of Health & Welfare, Republic of Korea (HN13C0078), and the 2018 Research Fund (1.180042.01) of UNIST.

VI. REFERENCES

[1] M. R. Pena Ferreira, P. C. Costa, and F. M. Bahia, "Efficacy of anti-wrinkle products in skin surface appearance: a comparative study using non-invasive methods," *Skin Res. Technol.*, vol. 16, pp. 444-449, 2010.
[2] M. Lodén, I. Buraczewska, and K. Halvarsson, "Facial anti-wrinkle cream: influence of product presentation on effectiveness: a randomized and controlled study," *Skin Res. Technol.*, vol. 13, pp. 189-194, 2007.
[3] "Anti-Aging Market by Demographics, by Products, by Services, by Devices, and by Region-Global Industry Analysis, Size, Share, Growth, Trends, and Forecasts (2016-2021)," Orbis Research, 2017.
[4] S. Sakai, M. Yamanari, Y. Lim, N. Nakagawa, and Y. Yasuno, "*In vivo* evaluation of human skin anisotropy by polarization-sensitive optical coherence tomography," *Biomed. Opt. Express*, vol. 2, pp. 2623-2631, 2011.
[5] G. L. Grove, M. J. Grove, and J. J. Leyden, "Optical profilometry: an objective method for quantification of facial wrinkles," *J. Am. Acad. Dermatol.*, vol. 21, pp. 631-637, 1989.
[6] P. M. Friedman, G. R. Skover, G. Payonk, A. N. Kauvar, and R. G. Geronemus, "3D in-vivo optical skin imaging for topographical quantitative assessment of non-ablative laser technology," *Dermatol. Surg.*, vol. 28, pp. 199-204, 2002.
[7] N. Iftimia, R. D. Ferguson, M. Mujat, A. H. Patel, E. Z. Zhang, W. Fox, and M. Rajadhyaksha, "Combined reflectance confocal microscopy/optical coherence tomography imaging for skin burn assessment," *Biomed. Opt. Express*, vol. 4, pp. 680-695, 2013.
[8] S. J. Lin, R. J. Wu, H. Y. Tan, W. Lo, W. C. Lin, T. H. Young, C. J. Hsu, J. S. Chen, S. H. Jee, and C. Y. Dong, "Evaluating cutaneous photoaging by use of multiphoton fluorescence and second-harmonic generation microscopy," *Opt. Lett.*, vol. 30, pp. 2275-2277, 2005.
[9] M. J. Koehler, K. König, P. Elsner, R. Bückle, and M. Kaatz, "*In vivo* assessment of human skin aging by multiphoton laser scanning tomography," *Opt. Lett.*, vol. 31, pp. 2879-2881, 2006.
[10] T. Fujimura, K. Haketa, M. Hotta, and T. Kitahara, "Global and systematic demonstration for the practical usage of a direct *in vivo*

This article has been accepted for publication in a future issue of this journal, but has not been fully edited. Content may change prior to final publication. Citation information: DOI 10.1109/JSTQE.2018.2873489, IEEE Journal of Selected Topics in Quantum Electronics

measurement system to evaluate wrinkles," *Int. J. Cosmet. Sci.*, vol. 29, pp. 423-436, 2007.

[11] M. C. Bloemen, M. S. van Gerven, M. B. van der Wal, P. D. Verhaegen, and E. Middelkoop, "An objective device for measuring surface roughness of skin and scars," *J. Am. Acad. Dermatol.*, vol. 64, pp. 706-715, 2011.

[12] U. Jacobi, M. Chen, G. Frankowski, R. Sinkgraven, M. Hund, B. Rzany, W. Sterry, and J. Lademann, "*In vivo* determination of skin surface topography using an optical 3D device," *Skin Res. Technol.*, vol. 10, pp. 207-214, 2004.

[13] D. Huang, E. A. Swanson, C. P. Lin, J. S. Schuman, W. G. Stinson, W. Chang, M. R. Hee, T. Flotte, K. Gregory, C. A. Puliafito, and et al., "Optical coherence tomography," *Science*, vol. 254, pp. 1178-1181, 1991.

[14] J. Welzel, E. Lankenau, R. Birngruber, and R. Engelhardt, "Optical coherence tomography of the human skin," *J. Am. Acad. Dermatol.*, vol. 37, pp. 958-963, 1997.

[15] T. Gambichler, V. Jaedicke, and S. Terras, "Optical coherence tomography in dermatology: technical and clinical aspects," *Arch. Dermatol. Res.*, vol. 303, pp. 457-473, 2011.

[16] M. Mogensen, L. Thrane, T. M. Jorgensen, P. E. Andersen, and G. B. Jemec, "OCT imaging of skin cancer and other dermatological diseases," *J Biophotonics*, vol. 2, pp. 442-451, 2009.

[17] M. T. Tsai, C. H. Yang, S. C. Shen, Y. J. Lee, F. Y. Chang, and C. S. Feng, "Monitoring of wound healing process of human skin after fractional laser treatments with optical coherence tomography," *Biomed. Opt. Express*, vol. 4, pp. 2362-2375, 2013.

[18] Y. Ahn, C. Y. Lee, S. Baek, T. Kim, P. Kim, S. Lee, D. Min, H. Lee, J. Kim, and W. Jung, "Quantitative monitoring of laser-treated engineered skin using optical coherence tomography," *Biomed. Opt. Express*, vol. **7**, pp. 1030-1041, 2016.

[19] T. Gambichler, R. Matip, G. Moussa, P. Altmeyer, and K. Hoffmann, "*In vivo* data of epidermal thickness evaluated by optical coherence tomography: effects of age, gender, skin type, and anatomic site," *J. Dermatol. Sci.*, vol. 44, pp. 145-152, 2006.

[20] M. A. Boone, M. Suppa, A. Marneffe, M. Miyamoto, G. B. Jemec, and V. Del Marmol, "High-definition optical coherence tomography intrinsic skin ageing assessment in women: a pilot study," *Arch. Dermatol. Res.*, vol. 307, pp. 705-720, 2015.

[21] S. Wu, H. Li, X. Zhang, and Z. Li, "Optical features for chronological aging and photoaging skin by optical coherence tomography," *Lasers Med. Sci.*, vol. 28, pp. 445-450, 2013.

[22] J. Weissman, T. Hancewicz, and P. Kaplan, "Optical coherence tomography of skin for measurement of epidermal thickness by shapelet-based image analysis," *Opt. Express*, vol. 12, pp. 5760-5769, 2004.

[23] G. Josse, J. George, and D. Black, "Automatic measurement of epidermal thickness from optical coherence tomography images using a new algorithm," *Skin Res. Technol.*, vol. 17, pp. 314-319, 2011.

[24] M. Ali and B. Hadj, "Segmentation of OCT skin images by classification of speckle statistical parameters," in *2010 IEEE International Conference on Image Processing (ICIP)*, pp. 613-616, 2010.

[25] A. Li, J. Cheng, A. P. Yow, C. Wall, D. W. Wong, H. L. Tey, J. Liu. "Epidermal segmentation in high-definition optical coherence tomography," 2015 Annual International Conference of the IEEE Engineering in Medicine and Biology Society (EMBC), pp. 3045-3048, 2015.

[26] F. Blateyron, "The Areal Field Parameters," in *Characterisation of Areal Surface Texture*, Springer Berlin Heidelberg, 2013, pp. 15-43.

[27] Z. Wang, B. Potsaid, L. Chen, C. Doerr, H. C. Lee, T. Nielson, V. Jayaraman, A. E. Cable, E. Swanson, J. G. Fujimoto, "Cubic meter volume optical coherence tomography," *Optica*, vol. 3(12), pp. 1496-1503, 2016.

[28] A. Taghavikhalilbad, S. Adabi, A. Clayton, H. Soltanizadeh, D. Mehregan, and M. R. N. Avanaki, "Semi-automated localization of dermal epidermal junction in optical coherence tomography images of skin," Appl. Opt., vol. 56, pp. 3116-3121, 2017.

[29] D. Xu, Y. Huang, and J. U. Kang, "Real-time compressive sensing spectral domain optical coherence tomography," *Opt. Lett.*, vol. 39, pp. 76-79, 2014.

[30] N. Iftimia, O. Yelamos, C. J. Chen, G. Maguluri, M. A. Cordova, A. Sahu, J. Park, W. Fox, C. Alessi-Fox, and M. Rajadhyaksha, "Handheld optical coherence tomography-reflectance confocal microscopy probe for detection of basal cell carcinoma and delineation of margins," *J. Biomed. Opt.*, vol. 22, pp. 76006, 2017.

Sanzhar Askaruly was born in Kazakhstan in 1994. He received B.S. degree in electrical and electronics engineering from Nazarbayev University, Kazakhstan in 2016. He is currently pursuing the M.S. degree in Biomedical Engineering at Ulsan National Institute of Science and Technology (UNIST), South Korea. His research interests include quantitative image processing and applications of deep learning for optical imaging.

Yujin Ahn received his B.S. degree from the Department of Bioengineering at the Ulsan National Institute of Science and Technology (UNIST) in 2014. Since 2014 he has studied in the Department of Biomedical Engineering at the UNIST for combined masters and Ph. D. program. From 2017, he has been an intern researcher at Center for Genomic Integrity in Institute for Basic Science (IBS). Main research interests are Optical Coherence Tomography (OCT), Tissue Engineering, and 3D Bio-printing.

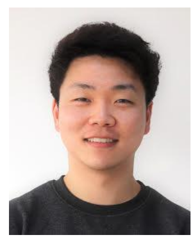

Hyeongeun Kim was born in South Korea, in 1992. He received B.S. degree in Biomedical Science and M.S. degree in Biomedical Engineering from Ulsan National Institute of Science and Technology (UNIST) in 2016 and 2018 respectively. Since 2017 he has been junior research engineer at SG Robotics, Seoul, South Korea. His research interests include enhancement of imaging depth with optical coherence tomography system and development of mobile biomedical sensor systems.

Andrey Vavilin received the B.S. degree in Applied Math from Novosibirsk State Technical University in 2004, and M.S. and Ph. D. degrees in Electrical Engineering from University of Ulsan, South Korea in 2007 and 2011 respectively. From 2013 to 2016 he was a researcher in Translational Biophotonics Lab at Ulsan National Institute of Science and Technology (UNIST), South Korea. Since 2016 he has been lead engineer in Video Analytics department of Atapy Software (Novosibirsk, Russia). His research interests include automatic video-analysis, biomedical imaging, machine learning and computer vision.

Sungbea Ban is bio-medical and optical imaging engineer working in the field of bio-photonics. Sungbea Ban received his Bachelor Degree in 2013 from the Department of Electrical and Computer Engineering at the University of Illinois at Urbana Champaign (UIUC). And he is currently pursuing his Ph. D. in Biomedical Engineering at Ulsan National Institute of Science and Technology (UNIST). He is interested in developing a new

kind of biomedical imaging tool and apply it to clinics. Main interests are Optical Coherence Tomography (OCT), Optical Projection Tomography (OPT), Diffraction Phase Microscopy (DPM), Histopathology, and Immunohistochemistry (IHC).

Pil Un Kim is an engineering researcher and researching professor in the fields of bio-medical imaging and system integrations. He received his Ph. D. degree in 2011 from the Department of Medical and Biological Engineering at Kyoungpook National University, and he is currently researching and developing optical and biological system in Institute of Biomedical Engineering at Kyungpook National University. Having experience in high performance system integration and development of OCT system for various applications, he is interested in translating new technologies from research to clinical and industrial applications. Main research interests are Biomedical device development, Optical Coherence Tomography (OCT) and Digital Image Processing.

Seunghun Kim received M.S. degree in Department of Biological Sciences, Korean Advanced Institute of Science and Technology (KAIST). And he is currently pursuing his Ph. D. in Department of Dermatology, College of Medicine, Chungang University. Started since 2002, he is currently a leader of Skin research institute, Amorepacific R&D Center. His major interests include skin evaluation, cosmetics and functional food.

Haekwang Lee received Ph. D. in Medical Science in 2006 from Department of dermatology, at Yonsei University. From 1993 to present, he is working at Skin Research Institute, Amorepacific R&D Center. He also worked as visiting researcher in Department of Dermatology, University of Wales College of Medicine (UK) in 1994. In 2010-2011 He worked as visiting researcher in Department of Biomolecular and Chemical Engineering at University of Illinois at Urbana-Champaign. His research interests are skin science, imaging, clinical research and cosmetics.

Woonggyu Jung received his Ph. D. in 2008 from the Department of Biomedical Engineering at the University of California, Irvine. From 2001 to 2008, he worked at the Beckman Laser Institute and Medical Clinic at UC Irvine, which is one of the world's top research organizations in laser treatment and diagnosis. He also worked at the Beckman Institute for Advanced Science and Technology at the University of Illinois at Urbana-Champaign since January 2009. He has joined the faculty of UNIST in 2012, and currently works as an associate professor of Department of Biomedical Engineering. He is also co-founder and CTO of start-up company, Conecson which is focused on the futuristic business regarding to mobile-based medical devices. Dr. Jung has a strong research background in optical imaging technologies including optical coherence tomography (OCT), multiphoton microscopy (MPM), and miniaturized optical imaging probes. His research interest is to develop new optical technologies that address challenges in clinical medicine, basic biological research and neuroscience. In previous work, he developed a successful optical platform for *in vivo* translational research, and has published more than 60 peer-reviewed journal papers in the field of biophotonics.